XVI International Conference on Computational Plasticity. Fundamentals and Applications
COMPLAS 2021
E. Oñate, D. Peric, M. Chiumenti and Eduardo de Souza Neto (Eds)

Effect of long-term pore pressure evolution on the integrity of cement plugs of abandoned oil wells in CCS sites

A. MARTÍNEZ*, J. LIAUDAT†, C.M. LÓPEZ* and I. CAROL*

* ETSECCPB (School of Civil Engineering)
Universitat Politècnica de Catalunya (UPC)
Campus Nord UPC, 08034 Barcelona
E-mail: ariadna.martinez.e@upc.edu, carlos.maria.lopez@upc.edu, ignacio.carol@upc.edu

† Faculty of Civil Engineering and Geosciences
Delft University of Technology
2628 CN Delft, The Netherlands
E-mail: j.liaudat@tudelft.nl

Key words : constitutive laws, interface elements, oilwell cement, CO_2, carbon capture and storage.

Abstract. In the context of Carbon Capture Storage (CCS) in abandoned hydrocarbon reservoirs, a preliminary study of the effects of pore pressure evolution on the integrity of oil-well cement seals is performed. A 2D cross-section of the sealed oil-well system (caprock-external cement sheath-steel casing-cement plug) is analysed along its service-life (injection/production activities and abandonment) using the Finite Element Method with zero-thickness interface elements to represent potential cracks. In particular, these elements are pre-inserted in the analysis in between the contacts of caprock-external cement sheath, external cement sheath-casing and casing-cement plug. The results presented show that, depending on the initial state and range of pressure evolution, the different interfaces considered may open or close in a non-trivial manner during the pressure return process. This seems to indicate the importance of considering carefully the pressure return process and subsequent effective stresses evolution in abandoned reservoirs recycled to CCS, in order to avoid that new cracks in well cement seals may lead to potential CO_2 leakage in the storage site.

1 INTRODUCTION

In Carbon Capture Storage (CCS) sites, an important element of risk to be considered is the integrity of the cement seals of the abandoned wells in the reservoir [1]. Well abandonment is the final stage of oil and gas wells lifecycle of construction, production and abandonment. The barrier system of abandoned wellbore mainly includes the cement sheath between the formation and the casing, and the cement plug in the casing. The main goal of abandonment procedure once the life of a well is completed is to maintain wellbore integrity for a long time to restore the natural integrity of the formation which have been crossed by the hole. In the case that the site has been reconverted to CCS, this is even more essential in order to prevent CO_2 leaks from the storage site. It is important to note that the stress state of the well cement seal can be affected by the long term changes in pore pressures that take place after the oil exploitation activities have stopped [2]. For example, slow pressure return around extraction wells (where the pore pressure had been subjected to a sustained reduction during long extraction periods) may cause a progressive increase of the effective stresses acting on the cement casing and plug, while the opposite can happen at injection wells.

In addition, these effects may be partially modified by the overall structural response due to the volume changes induced by the effective stress changes [3].

In this paper, a preliminary study of the effects of such stress changes on the potential integrity of a 2D cross-section of the sealed oil well system (caprock-external cement sheath-steel casing-cement plug) during its service-life (injection/production activities and abandonment) is presented. The study has been performed by means of Finite Element Method (FEM), including zero-thickness interface elements to represent potential cracks. These elements are pre-inserted in between the contacts of caprock-external cement sheath, external cement sheath-casing and casing-cement plug. In a first analysis, the interface elements are equipped with an elasto-plastic constitutive law that accounts for the softening of the material strength parameters due to the fracturing mechanical work. This law has been proved to accurately reproduce observed fracture propagation behaviour of quasi-brittle cement-based materials [4,5]. However, this law does not represent realistically the closure behaviour of existing fractures, which turn out to be a key factor in the analysis. For this reason, a second analysis is presented using a modified version of another interface constitutive model under development, which accounts for the reduction of the fracture normal stiffness using a damage formulation.

2 CONSTITUTIVE LAWS FOR ZERO-THICKNESS INTERFACE ELEMENTS

2.1 Elasto-plastic interface constitutive model

The existing fracture-based interface constitutive law is based on the theory of elasto-plasticity and it incorporates concepts of fracture mechanics and fracture energy. Its behaviour is formulated in terms of the normal and tangential stress components along the mid-plane of the interface elements, $\boldsymbol{\sigma} = [\sigma_N, \sigma_T]^t$, and the conjugate relative displacements $\boldsymbol{r} = [r_N, r_T]^t$ (^{t} = transposed). The interface fracture model is based on a hyperbolic cracking surface [4], Fig.1a. The corresponding yield (cracking) function F is defined in terms of normal and shear stresses and three geometric parameters: the uniaxial tensile strength (χ), the apparent cohesion (c) and internal friction angle ($tan\phi$). The algebraic expression of F is [4]:

$$F(\boldsymbol{\sigma}) = -(c - \sigma_N tan\phi) + \sqrt{\sigma_T^2 + (c - \chi tan\phi)^2} = 0 \qquad (1)$$

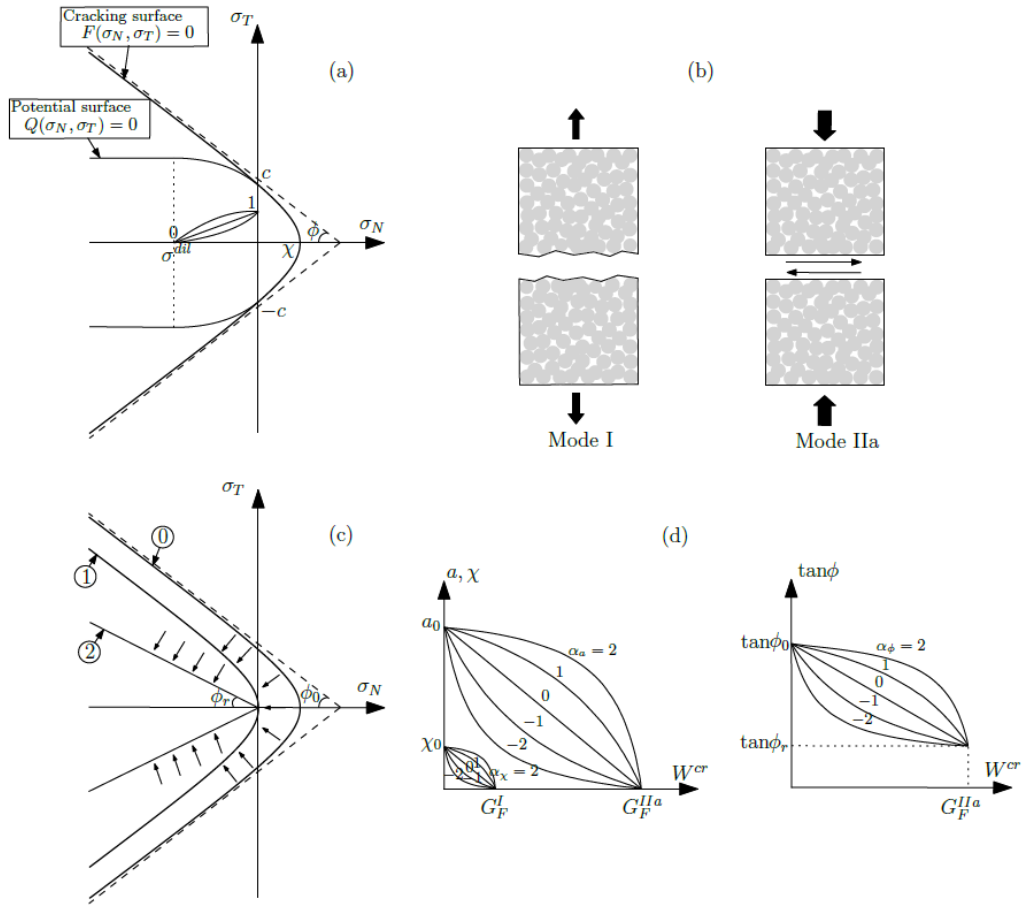

Figure 1: Interface model: (a) cracking surface and potential surface; (b) fundamental modes of fracture; (c) evolution of cracking surface; (d) softening laws for χ, a and $tan\phi$. Adapted from [4, 6].

The hardening/softening laws (evolution laws of the parameters of the fracture surface: χ, a and $tan\phi$) are formulated in terms of a single history variable, W^{cr}, defined as the energy spent in fracture processes. The variable a is the horizontal distance between the vertex of the updated hyperbola and its asymptotes. These laws, represented in Fig.1 (d), include as parameters the classical fracture energy in Mode I, G_f^I (pure tension) and a second mode of fracture, Mode IIa, defined as fracture under shear and high compression without dilatancy, with corresponding energy parameter G_f^{IIa} (Fig.1 (b)). The history variable evolution is defined incrementally as:

$$dW^{cr} = \begin{cases} \sigma_N dr_N^{cr} + \sigma_T dr_T^{cr} & if\ \sigma_N \geq 0\ (tension) \\ \sigma_T dr_T^{cr} \left(1 - \left|\frac{\sigma_N tan\phi}{\sigma_T}\right|\right) & if\ \sigma_N < 0\ (compression) \end{cases} \tag{2}$$

These expressions imply that, in tension, all work dissipated in the crack goes into the fracture process, while, in compression, the contribution to W^{cr} comes only from the shear work by subtracting the basic friction [4]. Note that, with the definitions above, the evolution of the cracking surface is as depicted in Fig.1c: from configuration "0" with initial tensile strength χ_0 and asymptotic cohesion c_0, as the history variable reaches $W^{cr} = G_f^I$ the surface moves to configuration "1" with zero tensile strength, and as it

approaches $W^{cr} = G_f^{IIa}$ the surface moves toward configuration "2" which correspond to a pair of straight lines of residual friction and no cohesion.

This elasto-plastic law is capable of representing most of the features of developing cracks under most loading scenarios [4]; however, it exhibits a limitation when simulating the behaviour of fractures under load-unload-reload cycles because unloading takes place with elastic stiffness, therefore potentially leading to premature unrealistic compression. This limitation may be avoided by using an alternative damage-frictional constitutive law with secant unloading which briefly outlined below.

2.2 Damage model

This model, which is currently under development in the MECMAT group at UPC [7], combines, a cohesive behaviour based on scalar damage theory, with basic frictional behaviour.

Scalar damage model

The elastic degradation of the stiffness matrix depends on the evolution of a single scalar damage variable L, according to the following expression :

$$\mathbf{K}^{sec} = e^{-L}\mathbf{K} \tag{3}$$

in which the initial elastic stiffness matrix $\mathbf{K}$ is a diagonal matrix with coefficients K_N and K_T in the normal and tangential direction respectively, and $\mathbf{K}^{sec}$ is the secant stiffness matrix. L is the logarithmic damage variable (internal variable) that leads to the evolution of the accumulated damage in the interface element, through the following expression:

$$D = 1 - e^{-L} \tag{4}$$

where D is the damage parameter, ranging between zero, for intact zone, and one for a completely damaged zone.

The fracture surface is the same as in the elasto-plastic law (Eq.(1)) but evolution laws of the surface parameters (χ, c and $tan\phi$) are modified. With the new evolution laws the initial cracking surface simply moves horizontally as a function of the damage parameter (D), reaching the final state of the hyperbola with vertex at the origin when $D = 1$ and the tensile strength is exhausted.

Frictional behaviour

A formulation based on the one proposed by [8] has been adopted considering that there is no degradation of the asperities (dilatancy is kept constant). The details of this formulation can be found in [7, 8], although this aspect of the formulation does not play a role in the present study.

2.3 Comparison of the constitutive laws

In order to illustrate the main differences in the behaviour of the elasto-plastic law and the damage-frictional law, a pure tension test with different load-unload-reload cycles is simulated. A single zero-thickness interface element is considered, with the following constitutive parameters: $K_N = K_T = 1000$ MPa/mm; $\chi_0 = 3$ MPa; $G_f^I = 0.03$ N/mm and

$G_f^{IIa} = 10G_f^I$. The unload-reload cycles are imposed at different points on the softening branch. Figure 2 shows the constitutive response of both laws. For the elasto-plastic law, the successive unload-reload cycles occur according to the initial elastic stiffness (Fig.2 (a)). In contrast, for the damage-frictional law, the successive unload-reload cycles occur according to secant stiffness, leading to a more realistic unloading. Note that, in the compression zone there is in any case a restitution of the initial stiffness (Fig.2 (b)).

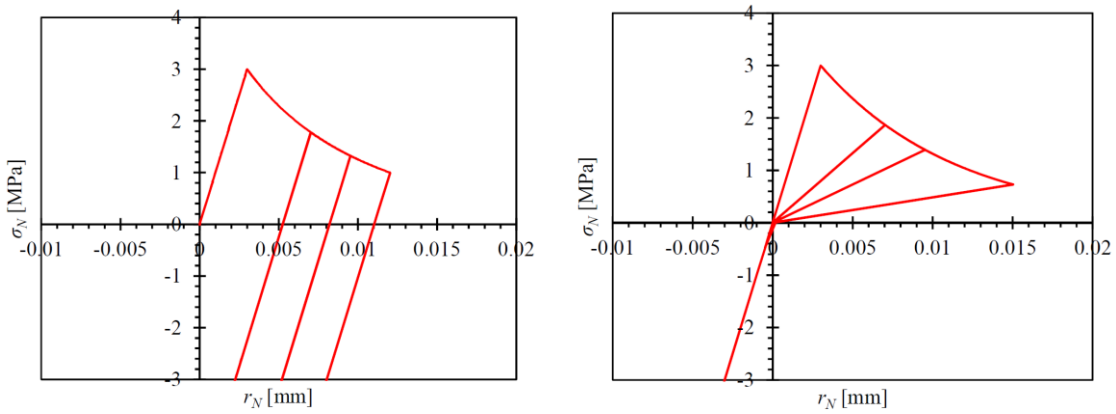

(a) Elasto-plastic law (b) Damage-frictional law

Figure 2: Pure tension test with load-unload-reload cycles. Normal stress versus normal relative displacement: (a) elato-plastic law and (b) damage-frictional law.

3 STRESS EVOLUTION AT THE MATERIAL INTERFACES OF A SEALED OILWELL

Conditions in a long-term reservoir show changes in pore pressure during injection/production activities and subsequent abandonment [2, 3]. The stress state of the well cement seal can be affected by the long term changes in pore pressures during its service life. Stress evolution can create cracks, especially at the contacts between caprock and cement sheath, between cement sheath and casing, and between casing and cement plug, and these cracks could eventually lead to CO_2 leakage in context of Carbon Capture and Storage.

The main objective of this study is to evaluate if, from a purely mechanical viewpoint, the expected stress changes may led to the opening and development of such cracks.

3.1 Model geometry and parameters

The geometry considered consists of a horizontal cross-section of the well system at the bottom level of the caprock. As shown in Fig.3 (left), three concentric circles configure the sealed oilwell system; starting from the centre these include: cement plug, steel casing, cement sheath and caprock. Due to the circular symmetry of geometry and loads, the analysis is run on one quarter of the well cross-section.

The analysis takes into account the construction sequence of the different components of the oilwell system, as illustrated in Fig.3 (right). Phase 1, when the well has not been perforated yet, corresponds to the caprock initial state. Phase 2, the well has been perforated but no casing has been installed yet. Phase 3, the cement sheath and steel

casing are installed. Finally, Phase 4, corresponds to the abandonment of the reservoir, when a cement plug has been placed to seal the well.

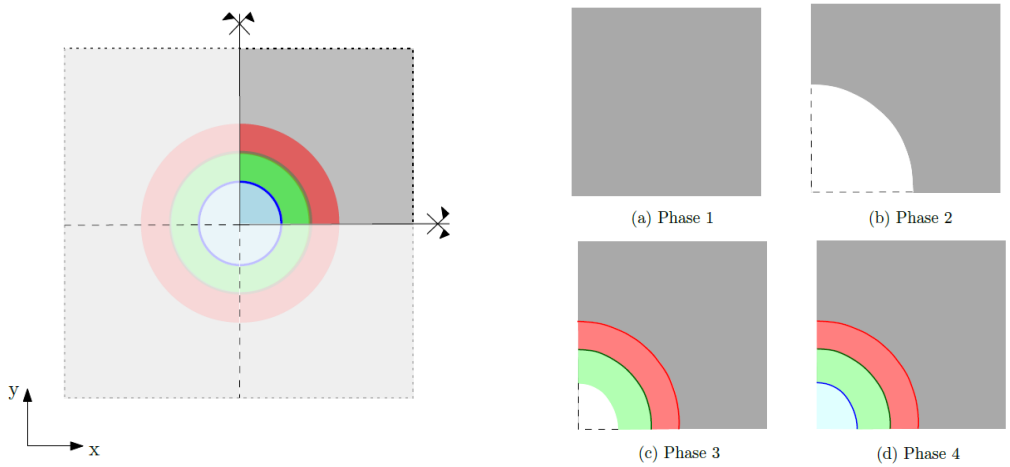

Figure 3: General geometry of the oilwell system (left image), and different phases in the construction sequence (right image).

For the FE analysis, the above geometry has been meshed with 751 quadratic triangular elements for the continuum medium. Along the contacts between different materials, 45 zero-thickness interface elements have been inserted to represent potential cracks (Fig.4). Continuum elements are assumed linear elastic (Table 1). Interface elements are equipped with the constitutive laws presented in Section 2, with the following parameters: $K_N = K_T = 10000$ MPa/mm; $\chi_0 = 1.2$ MPa; $c_0 = 2.5$ MPa; $tan\phi = 0.8$; $G_f^I = 0.03$ N/mm; $G_f^{IIa} = 10G_f^I$.

Table 1: Material properties of continuum

Material	Young Modulus [MPa]	Poisson's coefficient [-]
Caprock	20000	0.17
Cement	15000	0.20
Casing	210000	0.26

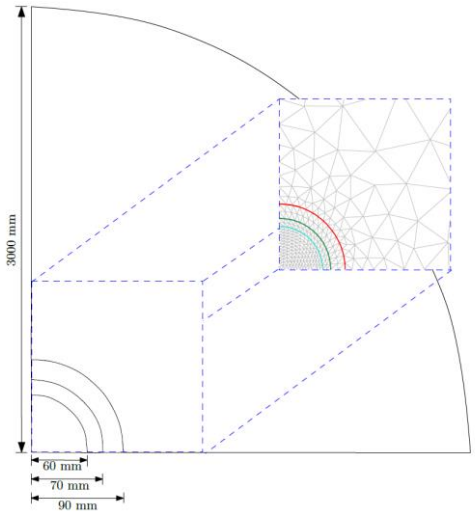

Figure 4: Geometry sketch and dimensions of the domain considered for the FE analysis, with detail of mesh used in the well area (different colours are used for the interface elements along the contacts between the different materials).

3.2 Boundary conditions

Given the purely mechanical nature of the model, the stress changes due to the variation of pore pressure in the reservoir will be simulated by means of changes in the values of the effective stresses applied as loads on the outer circular boundary. The boundary conditions are applied at each of the four stages of the construction sequence of Fig.5, are the following:

- Stage 1 (initial condition): corresponds to Phase 1 (Fig.5, right (a)), in which a uniform distributed load of 48 MPa is applied.
- Stage 2: corresponds to Phase 2 (Fig.5, right (b)), in which the distributed load is maintained (while, although not explicit in the figure, excavation of the inner hole implies the release of those stresses along the inner circular boundary).
- Stage 3 (injection activity): corresponds to Phase 3 (Fig.5, right (c)), in which once the casing and sheath cement have been placed, the load is linearly varied until the end of the stage by decreasing its value from 48 to 41 MPa (as a first simplified assumption, it is estimated that with the injection activity pore pressures around the well increase by 7MPa, and effective stress decrease by the same magnitude, without any structural redistribution effects).
- Stage 4 (abandonment): corresponds to Phase 4 (Fig.5, right (d)), in which once the cement plug has been placed, the load is linearly increased again by the same value of 7MPa, therefore returning effective stresses to the initial caprock conditions.

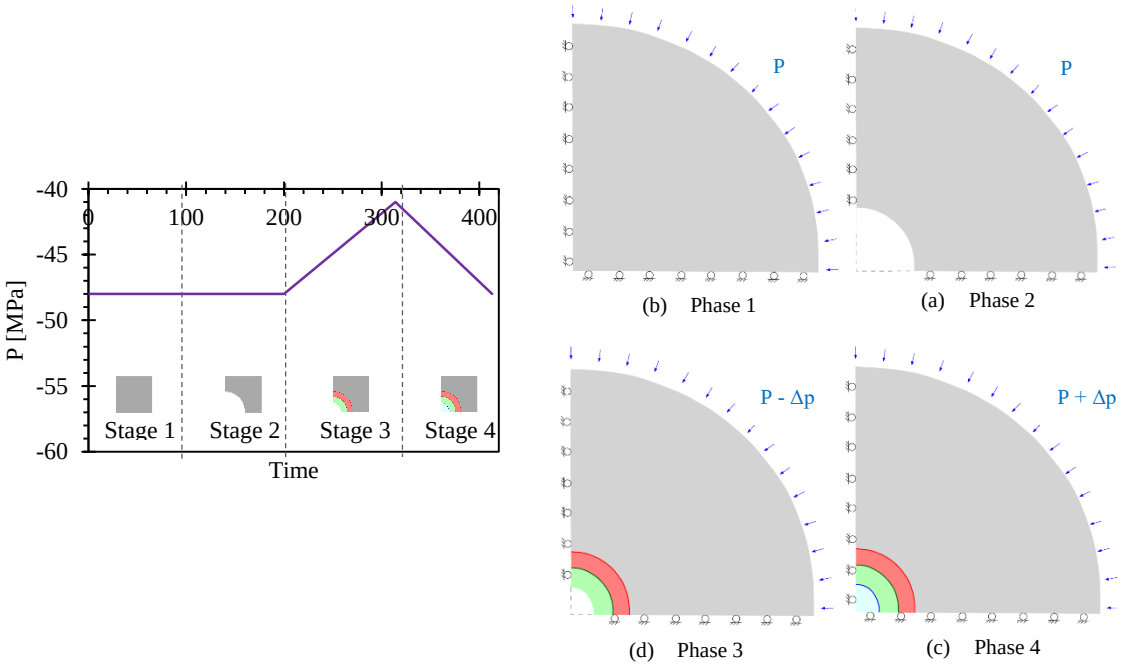

Figure 5: Time evolution of the external load (effective stresses) applied over the outer circular domain boundary (left diagram), an corresponding boundary conditions applied during the different construction stages of the analysis (right).

3.3 Results obtained with the elasto-plastic law

The diagram in Figure 6 (a) represents the time evolution of the normal stress obtained for each interface between continuum materials: caprock-cement joint (red line), cement-casing joint (green line) and casing-plug joint (blue line), during the stages considered. It can be appreciated that from stage 3, when the distributed load applied is linearly decreasing, due to the elevated reservoir pressures during injection activity, tensile stresses develop and cracks open along the caprock-cement interface (red) and the cement-casing interface (green). At the beginning of stage 4, however, this tendency is reversed and all interfaces (including the casing-plug interface that is incorporated only at this stage, in blue) change to compression.

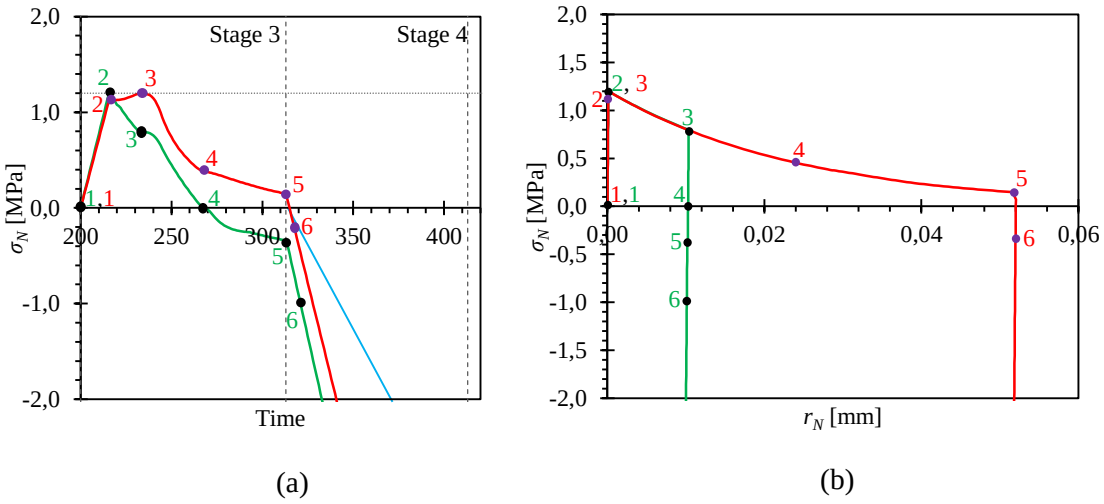

Figure 6: Results obtained with elasto-plastic law: (a) time evolution during the stages 3 and 4, of the normal stress obtained along the caprock-cement interface (red line), the cement-casing interface (green line) and the casing-plug interface (blue line), and (b) evolution of the stress-deformation state of the caprock-cement interface (red line) and cement-casing interface (green line).

To better understand the curves of Fig.6 (a), it is useful to represent the evolution of the various interface stresses on the corresponding constitutive diagram (normal stress-relative displacement diagram of Fig.6 (b)). There, it can be seen that stresses along the caprock-cement interface (red line) and cement-casing interface (green line) start evolving similarly, but the green line reaches the maximum strength slightly earlier, at Point 2. Then, the cement-casing interface already descends along the softening branch, while the caprock-cement interface is still in elastic state until it reaches the peak at Point 3. After that, tensile stress is reduced in both interfaces, but while the caprock-cement interface follows the softening branch until the end of the stage 3 (Point 5), the cement-casing interface unloads elastically until Point 4 when it goes into compressive values. From the stage 4 once injection stopped and pore pressure returning (Points 5 to 6) both interfaces goes into compression state. As it will be seen in the next section, the elastic unloading causes premature compressions and may be unrealistic.

3.4 Results obtained with the damage-frictional law

Figure 7 includes the results obtained with the damage-based interface law with secant unloading. The points marked in the diagrams designate the similar stages as in Fig.6. It can be seen that up to Point 3 the behaviour of both joints remains the same as the previous case with an elasto-plastic law. However, from this point, the evolution of

the cement-casing interface (green line) remains in the tensile zone during stage 3, and in stage 4 the stresses of the caprock-cement and cement-casing interfaces both vanish uniformly while the casing-plug interface never reaches cracking (Fig. 7 (a)). The caprock-cement interface has the same behaviour as in the previous case until Point 5 (end of stage 3), but the cement-casing interface enters into a secant unload state (towards the origin) until Point 5, leading to real unloading. Finally, once injection stopped until the end of the stage 4 where the initial condition is recovered, a secant unload is produced in both interfaces until the total closure of cracks, therefore not now developing any compression states of the two interfaces, which is a major difference to the results of the previous section using the elasto-plastic constitutive law.

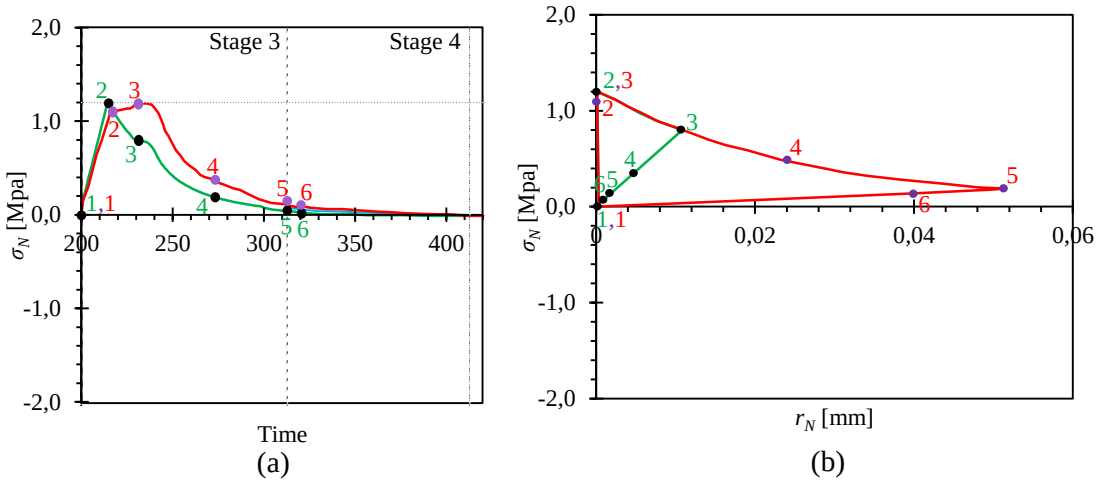

Figure 7: Results obtained with damage law: (a) time evolution during the stages 3 and 4, of the normal stress obtained along the caprock-cement interface (red line), the cement-casing interface (green line) and the casing-plug interface (blue line), and (b) evolution of the stress-deformation state of the caprock-cement interface (red line) and cement-casing interface (green line).

4 CONCLUDING REMARKS

- A preliminary study of the stresses evolution at the material interface of an oilwell casing and plug along its service life has been performed.
- In injection oilwells, the increase of pore pressure generates a decrease in effective stresses which, after stopping injections and sealing the oilwell, slowly recovers its initial conditions. This situation generates that, during the exploitation activity, the caprock-cement interface and cement-casing interface enter a state of cracking that, in their interaction, gives rise to the unload of the cement-casing interface while the caprock-cement interface remains in softening area. Regarding the pressure return phase, the trend is the opposite, that is, a decrease in pressure and an increase in effective stress, which tends to close the cracks opened in the previous stage.
- The interface elasto-plastic constitutive law cannot represent realistically the complete or partial closure of the cracks, the unloading occurs according to the magnitude of the elastic stiffness, leading to unrealistic compression.
- The interface damage-frictional law can represent more realistically the complete or partial closure of the cracks, the unloading occurs according to the lower magnitude of the (secant) stiffness, leading to more realistic unloading.

- In the analysis carried out, constant total stress conditions have been assumed, which in general may not occur. Lower or higher stresses caused by the opposite changes in the pore pressures may lead to expansion or contraction of the reservoir, thereby reducing or increasing stresses in the overlying caprock and possibly changing the local vertical stresses due to the arching effects. These structural effects have not been taken into account in this study.

ACKNOWLEDGMENTS

This research is supported by grants BIA2016-76543-R from MEC (Madrid), which includes FEDER funds, and 2017SGR-1153 from AGAUR (Generalitat de Catalunya, Barcelona). The first author thanks the scholarship 2017FI-B00559 received from AGAUR (Generalitat de Catalunya, Barcelona).

REFERENCES

[1] S.E. Gasda, S. Bachu, M.A. Celia, The potential for CO_2 leakage from storage sites in geological media; analysis of well distribution in mature sedimentary basins, *Environmental Geology* (2004) **46**(6-7)- 707-720.

[2] M. Mainguy, P. Longuemare, A. Audibert, E. Lécolier, Analyzing the risk of well plug failure after abandonment, *Oil & Gas Science and Technology-Revue de l'IFP* (2007) **62**(3):311-324.

[3] J. Rutqvist, D.W. Vasco, L. Myer, Coupled reservoir-geomechanical analysis of CO_2 injection and ground deformations at in Salah, Algeria, *International Journal of Greenhouse Gas Control* (2010) **4**(2):225-230.

[4] I. Carol, P. Prat, C.M. López, Normal/shear cracking model: application to discrete cracks analysis, *Journal of Engineering Mechanics* (1997) **123**(8):765-773.

[5] I. Carol, C.M. López, O. Roa, Micromechanical analysis of quasi-brittle materials using fracture interface elements, *International Journal Numerical Methods Engineering* (2001) **52**:193-215.

[6] C.M. López, I. Carol, A. Aguado, Meso-structural study of concrete fracture using interface element i: numerical model and tensile behaviour, *Materials and Structure* (2008) **41**(3):583-599.

[7] L. Puiggròs (2017) Modelo de comportamiento de juntas basado en la mecánica de daño, plasticidad y fractura. Master's thesis, Dept. of Geotechnical Engineering and Geo-Sciences, Universitat Politècnica de Catalunya (UPC), Barcelona.

[8] M. Snyman, J. Martin, A consistent formulation of a dilatant interface, *International Journal for Numerical Analytical Methods Geomechanics* (1992) **16**(7):493-527.